

Developmental long trace profiler using optimally aligned mirror based pentaprism

Samuel K. Barber

Lawrence Berkeley National Laboratory,

1 Cyclotron Road, M/S 2R0400,

Berkeley, CA 94720-8199, USA

+1-510-486-4077 TEL

+1-510-486-7696 FAX

Email address: SBarber@lbl.gov (currently at SBarber@physics.ucla.edu)

Gregory Y. Morrison

Lawrence Berkeley National Laboratory,

1 Cyclotron Road, M/S 2R0400,

Berkeley, CA 94720, USA

+1-510-486-4066 TEL

+1-510-486-7696 FAX

Email address: GYMorrison@lbl.gov

Valeriy V. Yashchuk

Lawrence Berkeley National Laboratory,

1 Cyclotron Road, 15R0317,

Berkeley, CA 94720, USA

+1-510-495-2592 TEL

+1-510-495-2742 FAX

Email address: VVYashchuk@lbl.gov

Mikhail V. Gubarev

NASA Marshall Space Flight Center (MSFC),

Huntsville, AL 35812, USA

+1-256-544-7816 TEL

Email address: mikhail.v.gubarev@nasa.gov

Ralf D. Geckeler

Physikalische-Technische Bundesanstalt,

Bundesallee 100,

38116 Braunschweig, Germany

+49 531 592-5220 TEL

+49 531 592-5205 FAX

Email address: ralf.geckeler@ptb.de

Jana Buchheim

Helmholtz Zentrum Berlin für Materialien und Energie, Elektronenspeicherring BESSY-II

Albert-Einstein-Str. 15,

12489 Berlin, Germany

+49 030 80621 5002 TEL

Email address: jana.buchheim@helmholtz-berlin.de

Frank Siewert

Helmholtz Zentrum Berlin für Materialien und Energie, Elektronenspeicherring BESSY-II

Albert-Einstein-Str. 15,

12489 Berlin, Germany

+49 030 8062 14846 TEL

Email address: frank.siewert@helmholtz-berlin.de

Thomas Zeschke

Helmholtz Zentrum Berlin für Materialien und Energie, Elektronenspeicherring BESSY-II

Albert-Einstein-Str. 15,

12489 Berlin, Germany

+ 49 030 8062 14745 TEL

Email address: thomas.zeschke@helmholtz-berlin.de

*Corresponding author: VYashchuk@lbl.gov

ABSTRACT

A low-budget surface slope measuring instrument, the Developmental Long Trace Profiler (DLTP), was recently brought into operation at the Advanced Light Source Optical Metrology Laboratory. The instrument is based on a precisely calibrated autocollimator and a movable pentaprism. The capability of the DLTP to achieve sub-microradian surface slope metrology has been verified via cross-comparison measurements with other high-performance slope measuring instruments when measuring the same high-quality test optics. In the present work, a further improvement of the DLTP is achieved by replacing the existing bulk pentaprism with a specially designed mirror based pentaprism. A mirror based pentaprism offers the possibility to eliminate systematic errors introduced by inhomogeneity of the optical material and fabrication imperfections of a bulk pentaprism. We provide the details of the mirror based pentaprism design and describe an original experimental procedure for precision mutual alignment of the mirrors. The algorithm of the alignment procedure and its efficiency are verified with rigorous ray tracing simulations. Results of measurements of a spherically curved test mirror and a flat test mirror using the original bulk pentaprism are compared with measurements using the new mirror based pentaprism, demonstrating the improved performance.

Keywords: surface metrology, surface profilometer, interferometric microscope, modulation transfer function, power spectral density, calibration, fabrication tolerances, metrology of x-ray optics

1. INTRODUCTION

A newly developed slope measuring instrument at the Advanced Light Source (ALS) Optical Metrology Lab (OML), the Developmental Long Trace Profiler (DLTP), has demonstrated a capability to reliably measure plane and slightly curved optics with an accuracy (absolute) of $<0.1 \mu\text{rad}$ and an accuracy of $<0.4 \mu\text{rad}$ for significantly curved optics.¹ The DLTP belongs to a class of optical deflectometric scanning devices that provides vital metrology for a range of optics including, but not limited to, X-ray optics found in synchrotron beamlines. With the continued evolution of third and fourth generation X-ray light sources requiring higher and higher quality optics with surface slope precision in the range of $0.1\text{-}0.2 \mu\text{rad}$,^{2,3} this class of instruments leads the way in providing the necessary metrology. To improve the versatility of the DLTP, modifications must be made allowing for higher accuracy measurements of curved optics.

The conception of the DLTP was based on the current highest performance slope measuring devices such as the Nanometer Optical Component Measuring Machine (NOM) at Helmholtz Zentrum Berlin (HZB)/BESSY-II (Germany)⁴⁻⁷ and the Extended Shear Angle Difference (ESAD) instrument at PTB (Germany).⁸⁻¹⁰ The common thread for each of these instruments is a precision calibrated electronic autocollimator and a scanning pentaprism (or optical square). In deflectometric scanning systems, pentaprisms have a well known and highly advantageous error minimizing property.

In order to totally realize the advantage, an original procedure for optimal alignment of a pentaprism in a deflectometric scanning system has been developed.¹¹ For an optimally aligned system, the pentaprism reduces the contribution of angular errors due, for example, to mechanical wobbling to only second order effects. It has been shown that by proper adjustment of the pentaprism, the influence of changes in angular orientation of the pentaprism can be

reduced by a factor of at least 1000 (on the order of a few nrad) for measurements along the tangential direction (along the direction of the scan measured by the vertical, V or Y , axis of the autocollimator) of a surface under test, SUT.

Despite the fact that precision fabricated pentaprisms offering down to 8 μ rad angular tolerances are commercially available, traditional “bulk” pentaprisms introduce undesirable systematic errors to slope measurements.¹ These errors are due to inhomogeneity of the bulk material from which they are fabricated and shape imperfections of the two reflecting and two refracting surfaces.

Conceptually, it is obvious that using a mirror based pentaprism can drastically improve the situation. With a mirror based pentaprism, the bulk material is entirely removed, as well as the refracting surfaces; and high quality flat mirrors provide the opportunity to significantly reduce the systematic errors due to the reflecting surfaces.

In the present work, we explore the opportunity to improve the performance of the DLTP¹ by replacing the bulk pentaprism currently in use with a mirror based pentaprism. We present a cost effective mechanical design of a mirror based pentaprism allowing for precise mutual alignment of the two mirrors – Sec. 2. We describe a corresponding alignment procedure and provide numerical simulation verifications of reliability and efficiency of the procedure – Sec. 3. Additionally, a modified alignment procedure suitable for alignment of mirror based pentaprisms of a different possible design⁵⁻⁷ is discussed in Sec. 3. It is shown that for the purpose of slope measurements via deflectometric scanning, the level of required precision for alignment of the two mirrors is significantly relaxed compared to the tolerances found in fabricated bulk pentaprism (Sec. 3.3). Development of a mirror based pentaprism for the ALS DLTP is described in Sec. 4. Finally, in Sec. 5 we compare surface slope measurements of a 15

m spherical mirror and a flat mirror made with the DLTP equipped with the developed and optimally aligned mirror based pentaprism and with the bulk pentaprism used in the instrument before the upgrade. In this way we determine the systematic error that has been removed along with the bulk pentaprism.

In the context of this paper, the term pentaprism (PP) refers to the bulk material pentaprism and the terms MBPP and optical square are used interchangeably for the mirror based versions of a pentaprism.

2. MIRROR BASED PENTAPRISM DESIGN

Figure 1 shows a design of a mirror based pentaprism developed at the ALS OML for use with the DLTP. In order to be an optical square arrangement, two mirrors must be precisely aligned with a declination angle of 45° . In the design shown in Fig. 1, the alignment is ensured with two kinematic mirror mounts for 1 inch optics attached to a specially designed pentagon base. The base cross-section looks like that which is used for a bulk pentaprism¹ with two orthogonal sides for input and output beams and two sides with the 45° declination where the mirrors on the kinematic stages are assembled. The kinematic stages for the mirrors provide all degrees of freedom that are necessary for an independent mutual alignment of the mirrors. Note that most of the parts used are ready to use opto-mechanical components available from Thorlabs, Inc.¹²

Similar to the existing bulk pentaprism mounting system used for the DLTP,¹ the assembly of the two mirrors with kinematic stages attached to the base is mounted to a rotatable kinematic platform. The mounting of the mirrors onto the additional kinematic platform facilitates the ability to execute the optimal pentaprism alignment procedure developed in Ref.¹¹ The procedure has been successfully applied to precisely align the DLTP bulk pentaprism.¹

A different style MBPP design is currently used in the NOM at BESSY-II,⁵⁻⁷ Fig. 2. The only difference is a lack of a third kinematic stage to adjust both mirrors as a single unit. In Sec. 3, an alternative alignment procedure is discussed for this particular design.

In the previous version of the DLTP,¹ a custom-made bulk pentaprism with a size of 30 mm \times 30 mm is used. In order to minimize the systematic error, five pentaprisms made of Homosil 101 were fabricated with the specified surface quality of $\lambda/10$, s/d 40/20, angle tolerance 3", and with anti-reflection coating on the two working surfaces. The pentaprisms were carefully tested with the ZYGOTM GPI interferometer and the best pentaprism was selected for the DLTP. Nevertheless, the quality of the DLTP pentaprism remained one of the major limitations of the instrumental performance.

Aiming for a cost effective solution for the MBPP, we use two 1 in. diameter gold coated mirrors selected from a set of 10 reasonably inexpensive mirrors from Thorlabs, Inc.¹² The mirrors are specified for surface quality $\lambda/10$. The selection is possible because we only need very high quality mirrors over a relatively small aperture. The selected mirrors have a flatness of about $\lambda/80$, peak-to-valley variation of ~ 8 nm and RMS height variation of ~ 1 nm over a 10 mm – in diameter – aperture. All parameters were measured with the ZYGOTM GPI interferometer available at the OML.

A major concern with the MBPP mirrors is the surface shape change due to mechanical stresses resulting from mounting the mirror substrates. To minimize the mounting stress, we attach the mirrors to the pentagon kinematic mount using a silicone rubber adhesive, RTV. This approach has been successfully used to mount mirrors of a high finesse power buildup cavity, developed for precision measurement of parity non-conservation in cesium.¹³ As it was shown in

Ref.,¹³ RTV adhesive is mechanically stable and does not relax (which can lead to misalignment of the mirrors).

The mirrors of the assembled MBPP were mutually pre-aligned with the ZYGOTM GPI interferometer, using a bulk pentaprism as a reference for 90 degree deflection of light beam. The final precision alignment was performed using a method discussed in the next section.

In order to compare the quality of the MBPP with the previous pentaprism of the DLTP, a test similar to one described in Ref.¹ was used. In the course of the test, a high quality plane reference mirror with $\lambda/40$ shape accuracy (~ 10 km radius of curvature and about 5 nm peak-to-valley height variation over 10 mm aperture) was measured with each pentaprism system placed in the interferometer beam path. The pentaprisms were mounted on the DLTP optical breadboard in order to make the test in an arrangement similar to their position in the DLTP. For the bulk pentaprism, the effective mirror shape looked like a smooth cylindrical surface (curved in the tangential direction) with a radius of curvature of approximately 350 m and peak-to-valley variation of about 310 nm (similar to the result obtained earlier in Ref.¹). The shape is a result of the optical path perturbation due to the double pass of the light beam through the pentaprism. With the MBPP, the reference mirror looked significantly smoother with overall radius of curvature larger than 9 km and peak-to-valley variation of about 15 nm.

3. ALIGNMENT PROCEDURES

In aligning the two mirrors of an MBPP (Fig. 3a), there are two primary errors, the wedge error, δ , and what we have chosen to call the parallel error, ϖ (Fig. 3b). The wedge error is easily visualized and understood; it's the deviation from the ideal wedge angle of 45° between mirrors M1 and M2 that produces the desired 90° deflection of the incoming beam. The parallel error is slightly more complicated to visualize. It is the difference in the roll angles of the M1

and M2 mirrors. Sufficiently minimizing the wedge error is straightforward and can be accomplished in a number of ways, which are discussed in Sec. 4.1, but minimizing the parallel error is more complex and requires a dedicated procedure. The following sections provide details for minimizing the parallel error for both the ALS OML and HZB/BESSY-II style MBPP designs. With the parallel and wedge error minimized, optimal alignment of the MBPP within a deflectometric scanning setup follows precisely the same procedure of Ref.¹¹ Both procedures assume that the MBPP is incorporated into an autocollimator based deflectometric scanning system and all components are aligned relative to the coordinate system of the autocollimator which is provided by its two perpendicular measuring axes and its optical axis.

3.1 Alignment procedure for an ALS style MBPP

The developed procedure, suitable for minimization of the parallel error of the ALS OML MBPP, can be graphically demonstrated via ray tracing simulations. Below we present the results of the rigorous ray tracing simulations. The simulation geometry, depicted in Fig. 4, represents the various degrees of freedom associated with the design shown in Fig. 1. For this system, any rotation of M2 can be expressed as a rotation of M1 without any loss of generality and so, for simplicity's sake, only independent rotations of the M1 mirror (in pitch with β_{M1} and in roll with α_{M1}) were considered in the simulation. Note that for the alignment procedure under discussion, the availability of third rotatable kinematic platform is crucial. The platform provides three rotational degrees of freedom for the MBPP unit as a whole: the roll α_{FP} , pitch β_{FP} , and yaw γ_{FP} – Fig. 3a.

Because this procedure relies heavily on the understanding of the procedure developed in Ref.,¹¹ it is prudent to introduce some of the concepts and terminology. The two most important concepts are the *yaw test* and *roll test*. These are the terms given to two unique procedures which

provide two parameters used to guide the optimal angular alignment of the pentaprism and of the surface under test (SUT) relative to the coordinate system of the autocollimator which is provided by its two perpendicular measuring axes and its optical axis. The first term, yaw test, refers to a series of measurements made in order to guide the optimal alignment of a reference flat SUT and autocollimator in relative roll angle. It is accomplished by adjusting the pentaprism about its yaw axis through a range of angles (about ± 4.8 mrad, this range of angles is chosen to match the measurement range of the autocollimator) and plotting the measured V (vertical angle) vs. H (horizontal angle) dependence. There is a linear relation between these two quantities; when the slope, M_{yaw} , is minimized, the relative roll angle between the SUT and autocollimator is also minimized. The second term, roll test, refers to series of measurements made in order to guide the optimal alignment of the pentaprism about its yaw axis. It is performed by adjusting the pentaprism about its roll axis and plotting the V vs. H dependence. There is a quadratic relation between these two quantities and the location of the vertex, H_{roll} , guides the alignment of the pentaprism about its yaw axis. The pentaprism is optimally aligned in yaw when $H_{roll} = 0$.

For the ALS OML style MBPP (Fig. 1), parallel error minimization is achieved through the following steps: with $M_{yaw} = 0$, a series of roll tests are performed in which the M1 mirror is successively rotated about its roll axis, α_{M1} . That is, a roll test is performed, then M1 is adjusted about α_{M1} and the roll test is repeated, thus yielding a series of quadratic dependences as shown in Fig. 4. The vertices of these quadratic dependences themselves exhibit a quadratic dependence. The vertex of this quadratic dependence occurs when the parallel error, ϵ , is equal to zero. With the parallel error equal to zero, the value of H_{roll} is then used to align the pentaprism unit about its yaw axis.

The ray tracing simulations also suggest that this procedure is insensitive to initial conditions. As such, this procedure offers a simple and easily executable method for minimizing the parallel error of an MBPP with a design like that which is discussed in Sec. 2.1. In Sec. 3.3 we will show that to reduce systematic errors of a movable pentaprism based slope measuring profiler to below 1 mrad, the parallel error need only be reduced to below 0.3 mrad. It is also shown in Sec. 4 that with the precision of adjustment of the newly fabricated MBPP at the ALS OML, the parallel error can be easily reduced to be below 0.1 mrad.

3.2 Alignment procedure for a HZB/BESSY-II style MBPP

The major difference between the HBZ/BESSY-II design for the MBPP and the ALS MBPP is the absence of a third kinematic platform to manipulate the MBPP as a single unit. As such, the traditional roll and yaw tests are not as easily executed. Accordingly, a different approach to the alignment is necessary. As with the preceding example, a procedure has been developed through rigorous ray tracing and verified through an analytic solution to the problem.¹⁴ The ray tracing simulation used for development of the BESSY-II style alignment procedure was written using the software FRED version 7.101.0.¹⁵ The simulation geometry is the same as that depicted in Fig. 3a. In contrast to the procedure discussed in Sec. 3.1, the BESSY-II procedure makes use of independent rotations of the M2 mirror.

To facilitate the description of this procedure some new terms are introduced. An M1 or M2 scan refers to a test, similar to the traditional roll test, in which the M1 or M2 mirror is rotated about its roll axis through a range of angles (about ± 4.8 mrad). The quadratic dependences of the measured (simulated) V vs. H values produce two parameters used for guiding alignment, H_1 and V_1 for an M1 scan and H_2 and V_2 for an M2 scan. These parameters represent the locations of the vertices of the quadratic dependences in both the H and V angles.

A SUT roll test consists of adjusting the SUT about its roll axis through a range of angles (about ± 4.8 mrad). There is a linear relation between the measured (simulated) V vs. H dependence with a slope M_{st} .

The alignment procedure, developed through ray tracing simulations, is as follows. The M2 scan is repeated as M1 is incrementally adjusted about its roll axis, with the goal to obtain $H_2 = 0$. With $H_2 = 0$ the SUT roll test is repeated while M2 is adjusted about its roll axis until $M_{st} = 0$. In this configuration, the MBPP is optimally aligned relative to the autocollimator with the parallel error equal to zero.

3.3 Effects of non zero parallel error

We performed a straightforward ray tracing analysis to establish the influences of a non zero parallel error on scanning deflectometric measurements. To do this we simulate DLTP measurements of a flat surface tilted in the tangential direction over a range of ± 5 mrad, corresponding to the measurement range of the autocollimator. In the simulated measurements we introduce different values of ϖ and compare the measured values against the “real” values for the slope. The difference between the “real” and measured angles is the error. Again, as has been noted earlier, a constant offset error over the range of measurements is irrelevant to these types of slope measurements. As such, the focus for these simulations is the peak-to-valley variation of the error over the ± 5 mrad range of the autocollimator axis which measures the tangential slope. For each value of ϖ it is assumed that the optimal alignment procedure from Ref.¹¹ has been carried out.

It was found that in the tangential direction (the DLTP scanning direction) the error variation is highly insensitive to ϖ . That is, the error variation is less than 5 nrad for values of ϖ up to 5 mrad. The same is not true for the sagittal direction. In the sagittal direction, the error

increases linearly for increasing ω at a rate of roughly 8 $\mu\text{rad}/\text{mrad}$. This is less significant since measurements in the sagittal direction are also limited by first order contributions from varying roll and yaw angles of the MBPP. However, it does reveal that the parallel error can be reduced such that the systematic error in the sagittal direction is less than other limiting factors.

The preceding simulations were performed assuming essentially unlimited precision in adjustment of the MBPP system. If limits on the precision of adjustment are considered, the results change slightly. For the kinematic stages used for assembling the MBPP, the error of adjustment is smaller than 0.1 mrad. When allowing for this level of uncertainty in the MBPP alignment, the error in the tangential direction is a bit more sensitive to ω increasing roughly linearly at a rate of approximately 3 nrad/mrad. Accordingly, reducing the parallel error to a level of 0.3 mrad suffices to achieve sub nrad performance in the tangential direction.

4. DEVELOPMENT OF A MBPP FOR THE ALS DLTP

A prototype MBPP according to the design in Sec. 2.1, Fig. 1, was fabricated for use with the ALS DLTP.¹ For the precision alignment of the MBPP, we follow the procedure described in Sec. 3.1. First, the yaw test was repeated until a sufficiently small value of $M_{\text{yaw}} = 50 \mu\text{rad}$ was obtained.

Before performing the series of roll tests geared to find the optimal alignment of the roll angles of M1 and M2, i.e. $\omega = 0$, additional practical experimental techniques were considered. The alignment procedure, discussed throughout the present work, requires continuous access to the inside of the DLTP hutch which strongly affects the stability of the instrument. As a result, the alignment performance is affected by instrumental drift. In order to reduce the spurious drift effect, we use a method developed in Ref.¹⁶ designed to minimize the effects of long term drifts by applying an optimal scanning strategy. According to the method,¹⁶ an arbitrary polynomial

order of drift can be suppressed by averaging a set of “forward” (F) and “backward” (B) measurements made in the appropriate sequence. Because the series of roll tests needed to be performed can become time consuming, long term drifts can adversely affect the measurements. Accordingly, the method from Ref.¹⁶ was adapted and applied to suppress such effects. A “forward” measurement indicates a positive rotation of the M1 mirror about its roll axis before the roll test and a “backward” measurement indicates a negative rotation of the M1 mirror about its roll axis. The series of roll tests was performed in a F-B-B-F-B-F-F-B sequence which is sufficient for suppressing up to third polynomial order drifts.

The result of first roll test in the series of roll tests is shown in Fig. 5a. Using a linear regression analysis, the vertices (also found via linear regression) from the individual roll tests were fit to a second order polynomial with the goal to find the value of H_{roll} for which the parallel error, ω , is zero. In order to avoid a problem with a biased estimation, the minimum of the function in Fig. 5b was found in two steps. First, a second order polynomial fit was performed using the original coordinate frame of the autocollimator, as it is shown in Fig. 5b, with the result $H_{\text{roll}} = 2.7$ mrad. Secondly, the fit was repeated with the coordinate system shifted by the value of $H_{\text{roll}} = 2.7$ mrad found in the first step. In this way the standard error was reduced by a factor of two to 0.18 mrad. To set the MBPP to optimal alignment, the M1 mirror was adjusted about its roll axis until $H_{\text{roll}} = 2.9$ mrad was obtained, which is within the standard error. This completes the minimization of the parallel error, ω . Finally, to finalize the optimal alignment of the MBPP unit relative to the autocollimator, the entire unit was adjusted about its yaw axis, γ_{FF} , until $H_{\text{roll}} = 0.02$ mrad.

Analytic derivations based on ray tracing results allow us to estimate the parallel error of the MBPP in its original state and provide a means to determine the uncertainty in the parallel

error. It was found that the initial parallel error (after assembling the MBPP) was $\omega = -4.7$ mrad. After the procedure has been applied the parallel error is minimized to $\omega = 0$ with an evaluated uncertainty of 0.33 mrad.

As a check of repeatability and reliability, the series of roll tests was repeated. This time the sequence of measurements was extended to include 16 roll tests in the order F-B-B-F-B-F-F-B-B-F-F-B-F-B-B-F, sufficient for suppressing up to 4th order polynomial drifts. The result is shown in Fig. 6. It was found that the parallel error is minimized for $H_{\text{roll}} = -0.04$ mrad with a standard error of 0.07 mrad. This value indicates a high degree of success in the previous adjustments, for which the final value was $H_{\text{roll}} = 0.02$, suggesting that the previous efforts to minimize the parallel error were successful.

Of course, the series of roll tests ruins the previous alignment and so the M1 mirror was adjusted with the goal to obtain $H_{\text{roll}} = -0.04$ mrad. In the final state $H_{\text{roll}} = -0.10$ mrad, which is within the standard error. In this state, the parallel error of the MBPP is zeroed with an evaluated uncertainty of 0.13 mrad.

The wedge error is dealt with in the following way. Using the bulk pentaprism and a reference flat, all of the components of the DLTP system are brought into optimal alignment. The bulk pentaprism is then replaced with the MBPP and either M1 or M2 is adjusted about its respective pitch axis until the autocollimator V readout is zeroed. In this way the wedge error of the MBPP is matched to that of the bulk pentaprism as a reference, which is specified at 15 μrad . The effects of small wedge errors are discussed in Ref.¹¹ It is shown that they introduce a nearly constant offset that is irrelevant to deflectometric scanning measurements as it merely introduces an overall tilt of the SUT.

It has been shown in Sec. 3.3 that reducing the parallel error to ~ 0.3 mrad combined with the optimal alignment procedure from Ref.¹ suffices for suppressing systematic errors due to misalignment to below 1 nrad in the tangential direction. The error is well below the typical noise level of an autocollimator. The systematic errors in the sagittal direction can be significantly suppressed by minimizing the parallel error; but other factors still limit the performance for measurements in this direction.

Using the above alignment methods for the MBPP, the wedge and parallel errors have been minimized with uncertainties of 30 μ rad and 130 μ rad, respectively. Accordingly, all systematic errors related to MBPP misalignments are eliminated.

Experimental realization of the procedure discussed in Sec. 3.2 is in progress at the ALS OML.

5. PERFORMANCE OF THE DLTP WITH THE NEW MBPP

5.1 DLTP measurement procedure

The design of the DLTP allows for a simple and repeatable interchange of pentaprism systems using two alignment preservation pins. It was experimentally verified that the design provides a negligible change in angular orientation of the pentaprism system (bulk or MBPP) relative to the autocollimator after removal from and reintegration into the DLTP. Therefore, once the pentaprism (bulk or MBPP) has been optimally aligned, realignment of the pentaprism after removing from and reintegrating into the DLTP is unnecessary.

For making the highest quality measurements with the DLTP, we use a well defined strategy, which allows for significant suppression of the measurement errors due to systematic effects and instrumental and setup drifts.^{1,16,17} The strategy is briefly summarized here. Four measurements, each consisting of 8 traces, of the SUT performed in the forward/backward

sequence appropriate for drift error suppression,¹⁶ are made. After the first measurement (consisting of 8 traces), the SUT pitch angle is increased by 140 μrad and re-measured. Averaging the first two measurements suppresses systematic oscillations due to internal reflections within the autocollimator.¹ Additional suppression of an instrumental systematic error which is symmetric with respect to the mirror center, is achieved by averaging measurements performed with different orientations of the SUT with respect to the scanning direction.¹⁶ Thus, the third and fourth measurements are performed with the SUT rotated 180° about the axis of the probing beam. Again, a difference in SUT pitch of approximately 140 μrad is introduced between the third and fourth measurements. The first two measurements are said to be made with a forward orientation of the SUT while the third and fourth measurements are said to be made in a reversed orientation of the SUT. The final slope trace of the SUT is found as the average of all four measurements.

5.2 Measurements of a flat mirror

The first test of the performance of the DLTP equipped with the MBPP was to cross check measurements of a high quality flat mirror with DLTP measurements of the same surface made while equipped with the pentaprism. The results of these measurements, which were performed according to the strategy outlined in Sec. 5.1, are shown in Fig. 7. In the case of the pentaprism, the measured radius of curvature of the SUT was -197.24 km with an RMS slope variation of 0.17 μrad . For the MBPP, the measured radius was -142.35 km with an RMS slope variation of 0.14 μrad . A negative radius of curvature indicates a convex surface. The measurements produce nearly identical slope traces, as evidenced by Fig. 7a. The slight discrepancy in the measured radius is probably due to the significant difference of effective curvatures of the bulk (350 m) and mirror based pentaprisms (9 km), discussed in Sec. 2. Indeed,

in the case of the bulk pentaprism, even for a flat mirror, a small misalignment between the DLTP translation axis and the axis of the autocollimator light beam will lead to a noticeable error in the measurement of the mirror's curvature. Assuming the difference in the radius measurements made using the pentaprism and MBPP is due the pentaprism's significantly shorter effective radius, we conclude there is a 0.3 mrad misalignment in the vertical direction between the translational axis of the DLTP and the autocollimator axis. In the case of the mirror based pentaprism developed for the DLTP, the sensitivity to this type of misalignment is suppressed by a factor of approximately 25.¹⁴

The misalignment between the DLTP translational and optical axes, discussed above, which leads to a small variation of the optical path through the pentaprism, can interfere with the inhomogeneity of the bulk material, leading to a noticeable systematic error that is not completely removed with the measurement strategy described in Sec. 5.1.

The difference between measurements of the flat SUT made with the pentaprism and MBPP is shown in Fig. 7b. The RMS slope variation of this difference is 0.12 μ rad, which is rather small. This difference shows that, aside from some slight low order fluctuations, which are probably attributable the combination of the relatively large effective curvature of the pentaprism and a misalignment between the DLTP translation and autocollimator axes, there is no major systematic difference between the two systems.

Furthermore, in the case, of these measurements, the environmental control system was switched off, leading to temperature variations on the order of a degree Celsius over the course of single 8 scan measurement. In addition, the shifting mass of the scanning pentaprism unit combined with the large temperature variations leads to deformation of the relatively thin (5 mm) breadboard of the optical table. The small variation in the difference of the two measurements of

the flat SUT demonstrates that all of these significant environmental factors are handily averaged out by the measurement strategy (Sec. 5.1).

5.3 Measurements of 15 m spherical reference mirror

A set of cross-comparison DLTP measurements of a high quality 15 m reference mirror¹ supplied by InSync, Inc.¹⁸ were made using both the pentaprism and the ALS OML MBPP prototype. The 15 m spherical mirror allows for full characterization of DLTP performance over the entire dynamic range of the autocollimator, which is ± 4.8 mrad.

The above measurement strategy (Sec. 5.1) was carried out for measurements of the 15 m spherical mirror using the DLTP equipped with both pentaprism systems. The residual slope traces obtained after removing the best fit spherical surface shape are shown in Fig. 8a. In the case of the pentaprism the radius of curvature was measured at 14.975 m with RMS slope variation of 0.52 μ rad. For the MBPP, the measured radius was 14.987 m with RMS slope variation of 0.40 μ rad. Note that measurements made with the pentaprism are in excellent agreement with the same measurements made in Ref.,¹ in which the measured radius was 14.977 m, demonstrating a high degree of repeatability of DLTP measurements.

In the case of measuring a curved optic, the optical path through the pentaprism or MBPP will change significantly. By design, the MBPP has no systematic error resulting from bulk material. Moreover, the effective curvature of the MBPP, measured with the ZYGOTM GPI interferometer (Sec. 2), is improved by an order of magnitude compared with that of the bulk pentaprism. In Sec. 3 it was also shown that the residual misalignments in the MBPP have an entirely negligible effect on measurements. As a result, the difference of the measurements made with the pentaprism and MBPP yields the systematic error directly related to the inhomogeneous bulk material and the substantially worse effective surface shape of the pentaprism, Fig. 8b. In

fact, we performed a study to understand the effect of the effective radius of curvature of the pentaprism on DLTP measurements. We found that for the pentaprism with a radius of curvature of 350 m, over the range of the autocollimator (± 4.8 mrad) there should be a linear error term of $1.1 \mu\text{rad/mrad}$.¹⁴ This corresponds to a total change of $10 \mu\text{rad}$ over the autocollimator range. The difference of the pentaprism and MBPP DLTP measurements of the 15 m mirror (Fig. 8b) shows a total change of $7.5 \mu\text{rad}$. The slight difference between theory and experiment can be explained by noting that the calculations assume an effective shape of the pentaprism which is ideally spherical. In comparing the pentaprism system to the MBPP system we see almost exactly what we expect to see when comparing the pentaprism system to an ideal system. This leads to two important conclusions: theory and experiment are in agreement and the new MBPP system is a nearly ideal system. The DLTP equipped with the MBPP leads to a significant improvement in the accuracy of measurements of surface curvature. The corresponding performance can be characterized with a limit on spurious curvature due to the MBPP that is less than 10^{-4} km^{-1} ($R > 10,000 \text{ km}$). Note that the overall performance of the DLTP with regards to curvature measurements is significantly worse because of the lack a DLTP calibration that depends on distance between the autocollimator and the surface under test.^{1,19}

Of course, the difference in Fig. 8b exhibits some non linear behavior not predicted by our calculations. This is most likely related to higher order variations in the effective shape (including inhomogeneity of the PP material) of the pentaprism.

While replacing the DLTP pentaprism with an MBPP has removed a significant systematic error, a non negligible systematic error persists. Figure 9 shows the symmetrical systematic error determined as one half of the difference between the forward orientation and reverse orientation measurements performed with the MBPP. Note that an asymmetrical

systematic error cannot be removed by flipping the SUT orientation. One of the possible sources of this systematic error is the limited reliability (mentioned above) of the autocollimator calibration for varying optical path lengths as well as other external factors.¹⁹ This provides further evidence for the need to develop the universal test mirror (UTM) as proposed in Ref.²⁰

6. CONCLUSION

The impetus of this project was to improve the DLTP slope measuring device by replacing the bulk pentaprism in favor of a mirror based alternative. Elimination of complexities due to the inhomogeneous bulk material and a significant improvement of the effective shape of the pentaprism are achieved with the MBPP.

Precise alignment procedures for two MBPP designs have been proposed. The procedure developed for the ALS OML style design has been verified through successful alignment of the prototype MBPP. Though the alignment procedures provide the means for very precise alignment of the two mirrors (~ 0.1 mrad), additional theoretical considerations have demonstrated that the optimal alignment procedure presented in Ref.¹¹ sufficiently suppresses systematic errors due to a non ideal optical square, thus relaxing the burden of precision alignment.

Measurements of a high quality flat optic allowed for the estimation of error associated with misalignment of the DLTP translational and optical axes, which is shown to be noticeable. (Work on precision mutual alignment of the of the DLTP translational and optical axes is in progress.) These measurements also demonstrate the effectiveness of the measurement strategy in suppressing significantly varying environmental conditions. The measurements of a significantly curved optic (15 m spherical mirror) have allowed for characterization of the DLTP performance over its entire measurement range. The difference of measurements made using the

bulk pentaprism and MBPP has revealed a strong systematic error associated with the bulk pentaprism which is removed when using the MBPP.

Summarizing, the performed investigations have significantly improved the reliability of the DLTP measurements. For the measurements with flat and slightly curved optics, the overall absolute accuracy is very close to the limit set by the specified repeatability of the autocollimator of 50 nrad. However, in order to reach a similar level of accuracy with significantly curved optics, a precise calibration of the DLTP (as well as any autocollimator based deflectometric scanning system, including NOM and ESAD) must be developed. A suitable calibration method that accounts for the dependence of calibration on variation of the optical path length has been proposed in Ref.²⁰ and it is under development.

ACKNOWLEDGEMENTS

The Advanced Light Source is supported by the Director, Office of Science, Office of Basic Energy Sciences, Material Science Division, of the U.S. Department of Energy under Contract No. DE-AC02-05CH11231 at Lawrence Berkeley National Laboratory.

DISCLAIMER

This document was prepared as an account of work sponsored by the United States Government. While this document is believed to contain correct information, neither the United

States Government nor any agency thereof, nor The Regents of the University of California, nor any of their employees, makes any warranty, express or implied, or assumes any legal responsibility for the accuracy, completeness, or usefulness of any information, apparatus, product, or process disclosed, or represents that its use would not infringe privately owned rights. Reference herein to any specific commercial product, process, or service by its trade name, trademark, manufacturer, or otherwise, does not necessarily constitute or imply its endorsement, recommendation, or favoring by the United States Government or any agency thereof, or The Regents of the University of California. The views and opinions of authors expressed herein do not necessarily state or reflect those of the United States Government or any agency thereof or The Regents of the University of California.

References

1. V. V. Yashchuk, S. K. Barber, E. E. Domning, J. L. Kirschman, G. Y. Morrison, B. V. Smith, F. Siewert, T. Zeschke, R. D. Geckeler, and A. Just, "Sub-microradian Surface Slope Metrology with the ALS Developmental Long Trace Profiler," *Nucl. Instr. and Meth. A* **616**, 212-223 (2010).
2. L. Assoufid, O. Hignette, M. Howells, S. Irick, H. Lammert, and P. Takacs, "Future metrology needs for synchrotron radiation grazing-incidence optics," *Nucl. Instr. and Meth. A* **467-468**, 267-70 (2001).
3. P. Z. Takacs, "X-ray optics metrology," in M. Bass (Ed.), *Handbook of Optics*, third ed., vol. V, chapter 46, McGraw-Hill Publishing Company, New York (2009).
4. E. Debler, K. Zander, Ebenheitsmessung an optischen Planflächen mit Autokollimationsfernrohr und Pentagonprisma, PTB Mitteilungen Forschen + Prüfen, Amts und Mitteilungsblatt der Physikalisch Technischen Bundesanstalt, Braunschweig und Berlin, 339-349 (1979).
5. F. Siewert, T. Noll, T. Schlegel, T. Zeschke, and H. Lammert, "The Nanometer Optical Component Measuring machine: a new Sub-nm Topography Measuring Device for X-ray Optics at BESSY," *AIP Conference Proceedings* **705**, 847-850 (2004).
6. H. Lammert, T. Noll, T. Schlegel, F. Siewert, and T. Zeschke, Optisches Messverfahren und Präzisionsmessmaschine zur Ermittlung von Idealformabweichungen technisch polierter Oberflächen, Patent No.: DE 103 03 659 (28 July 2005).
7. F. Siewert, H. Lammert, and T. Zeschke, "The Nanometer Optical Component Measuring Machine," *Modern Developments in X-ray and Neutron Optics*, Springer-Verlag, Berlin/Heidelberg, (2008).

8. R. D. Geckeler, and I. Weingärtner, "Sub-nm topography measurement by deflectometry: flatness standard and wafer nanotopography," *Proc. SPIE*, **4779**, 1-12 (2002).
9. J. Illema, and M. Wurm, "Deflectometric Measurements of Synchrotron-Optics for Postprocessing," *AIP Conference Proceedings* **705**, 843-846 (2004).
10. R. D. Geckeler, "ESAD Shearing Deflectometry: Potentials for Synchrotron Beamline Metrology," *Proc. SPIE* **6317**, 1-12 (2006).
11. R. D. Geckeler, "Optimal use of pentaprisms in highly accurate deflectometric scanning," *Meas. Sci. Technol.* **18** 115-125 (2007).
12. www.thorlabs.com
13. C. S. Wood, S. C. Bennett, J. L. Roberts, D. Cho, and C. E. Wieman, "Precision Measurement of Parity Nonconsequence in Cesium," *Can. J. Phys.* **77**, 7-77 (1999).
14. S. K. Barber, R. D. Geckeler, V. V. Yashchuk, M. V. Gubarev, J. Buchheim, F. Siewert, and T. Zeschke, "Optimal Alignment of Mirror Based Pentaprism," (submitted 2010).
15. Photon Engineering, LLC, www.photonengr.com
16. V. V. Yashchuk, "Optimal Measurement Strategies for Effective Suppression of Drift Errors," *Rev. Sci. Instrum.* **80**, 115101/1-10 (2009).
17. J. L. Kirschman, E. E. Domning, W. R. McKinney, G. Y. Morrison, B. V. Smith, and V. V. Yashchuk, "Performance of the upgraded LTP-II at the ALS Optical Metrology Laboratory," *Proc. SPIE* **7077**, 1-12 (2008).
18. www.insyncoptics.com
19. R. D. Geckeler, A. Just, M. Krause, and V. V. Yashchuk, "Autocollimators for Deflectometry: Current Status and Future Progress," *Nucl. Instr. and Meth. A* **616**, 140-146 (2010).

20. V. V. Yashchuk, W. R. McKinney, T. Warwick, T. Noll, F. Siewert, T. Zeschke, and R. D. Geckeler, "Proposal for a Universal Test Mirror for Characterization of Slope Measuring Instruments," *Proc. SPIE* **6704**, 1-12 (2007).

Figures

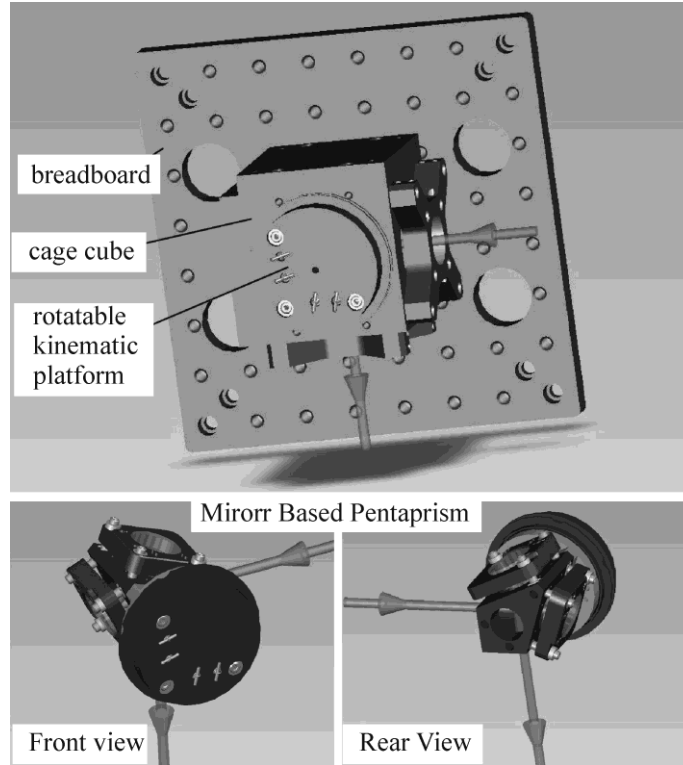


Figure 1: Design of the OML mirror based pentaprism. Most of the parts used are ready to use opto-mechanical components available from Thorlabs, Inc.¹²

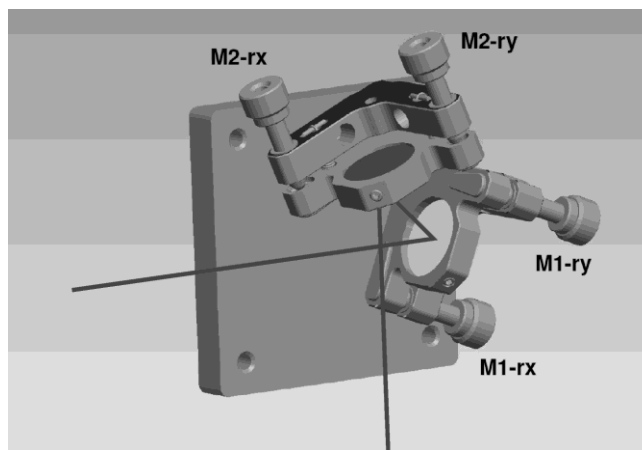


Figure 2: HZB/BESSY-II MBPP design scheme currently used in the NOM.

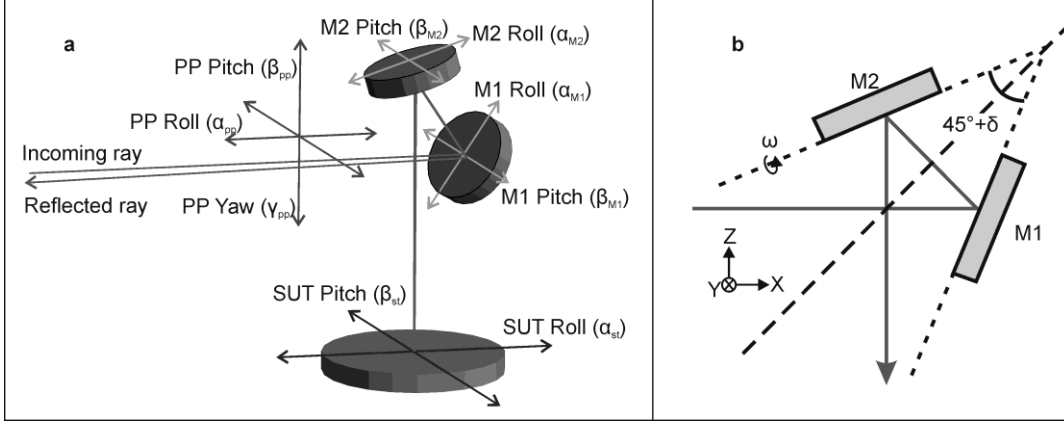


Figure 3: (a) Geometrical representation of the simulated MBPP and surface under test (SUT) system with the relevant coordinate systems. M1 and M2 can be rotated about two axes (M1 and M2 pitch and roll axes), the SUT can be rotated about two axes (SUT pitch and roll axes), and M1 and M2 can be rotated simultaneously about three axes (PP pitch, roll and yaw axes). The deviation of the reflected ray is calculated, simulating an autocollimator measurement. (b) Illustration of the wedge and parallel errors involved in an optical square.

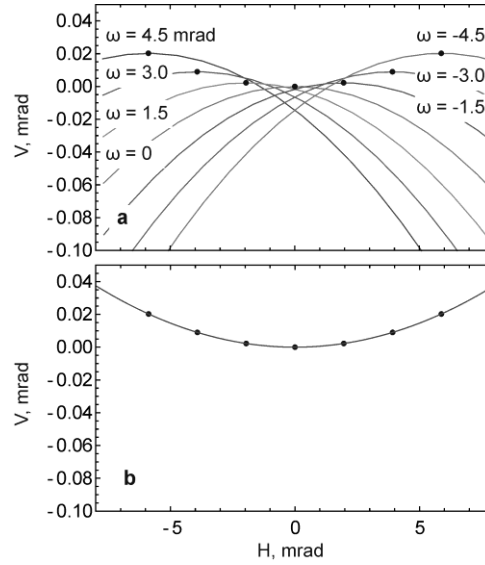


Figure 4: (a) Simulation results of applying a series of roll tests after successively incrementing the parallel error by adjusting the M1 mirror about its roll axis; and (b) a plot of the vertex points with a quadratic fit. The minimum of the quadratic fit in (b) occurs when the parallel error is equal to zero.

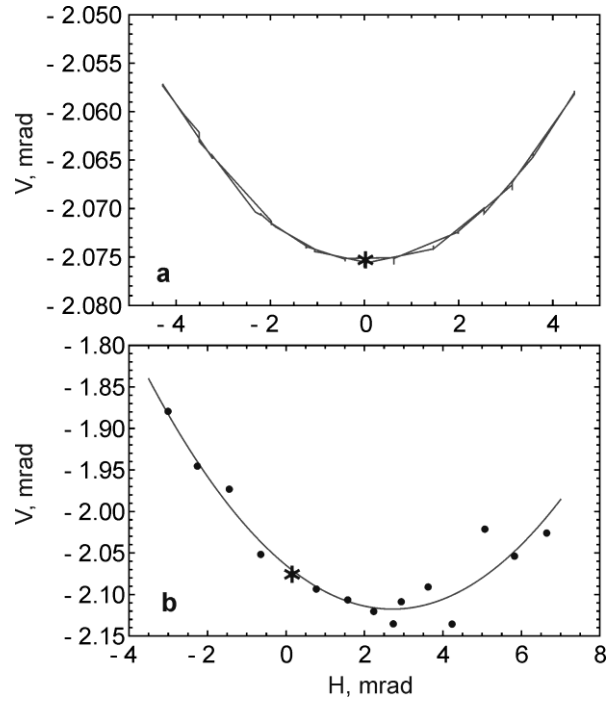


Figure 5: Single roll test with the vertex marked with an asterisk, taken from the series of roll tests performed as M1 is adjusted about its roll axis (a). Quadratic fit of the vertices found from the series of roll tests. The vertex shown in (a) with an asterisk is shown with an asterisk in (b). The parallel error is minimized when $H_{roll}=2.7$.

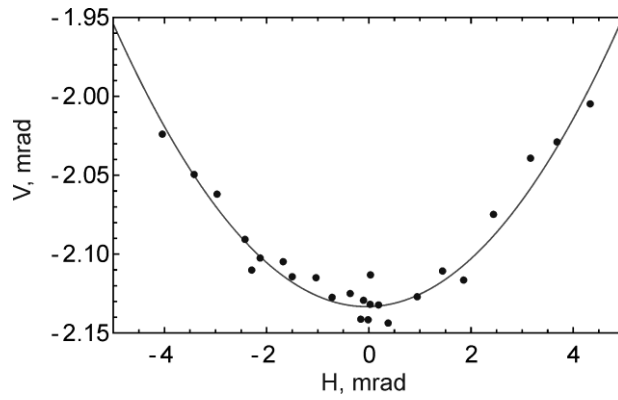


Figure 6: Series of roll tests repeated, demonstrating reliability and repeatability of the developed alignment procedure.

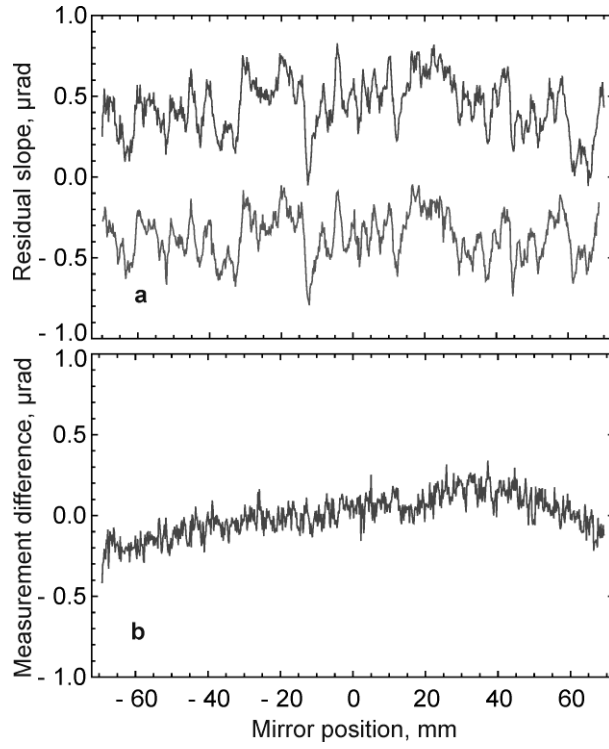


Figure 7: Residual slope traces of flat mirror (a) measured with DLTP equipped with MBPP (bottom line) and pentaprism (top line). The offset is introduced. Difference in the two sets of measurements (b).

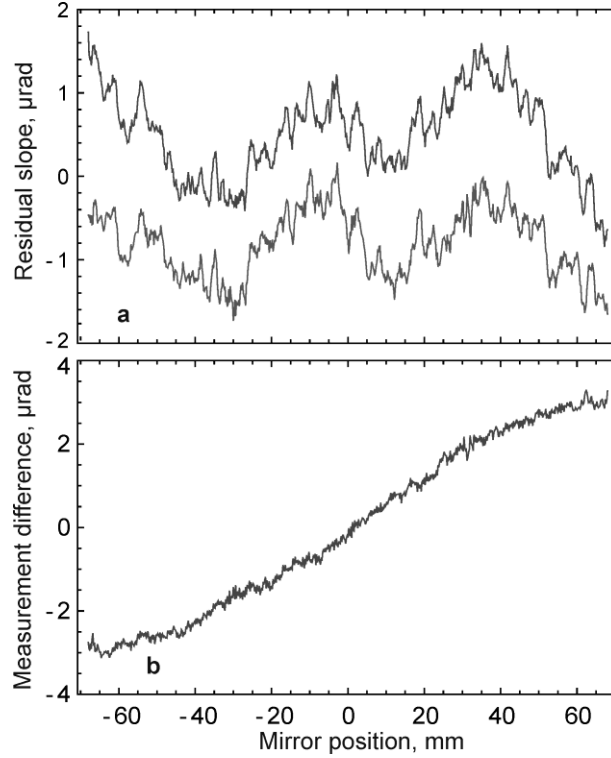


Figure 8: Slope traces of 15 m spherical mirror (a) measured with DLTP equipped with MBPP (bottom line) and pentaprism (top line). Offset is introduced. Difference in the two sets of measurements (b) which represents systematic error associated with bulk pentaprism.

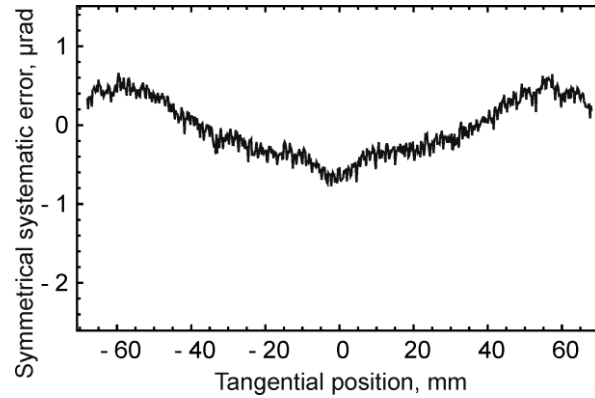


Figure 9: Half of difference between the forward and reverse measurements of the 15 m optic made with the DLTP equipped with the MBPP. This represents the symmetric error which is removed by averaging the forward and reverse measurements.